


Multistep polarization switching and reduced coercive field in lead titanate thin filmsYanzhe Dong and Xiaoyan Lu ^{*}*School of Civil Engineering, Harbin Institute of Technology, Harbin 150001, China*

(Received 11 March 2024; accepted 6 May 2024; published 3 June 2024)

Switchable polarization makes ferroelectric materials widely usable in nonvolatile memories and electronic nanodevices. The coercive electric field, determining the polarization switching, is crucially important for the design and usage of ferroelectric devices. To prevent leakage and dielectric breakdown of the devices, it is necessary to reduce the coercive electric field. In this work, we propose a theoretical model to study the domain switching properties of epitaxial PbTiO₃ films within the framework of Landau's phenomenological theory, especially the multistep polarization switching in ferroelectric thin films near a phase boundary. Results indicate that substrate strains can significantly affect the domain structures and the domain switching process. Under specific substrate strain conditions (tensile misfit strain of 0%–0.8%), polydomains exist and 180° polarization switching can be achieved via a two-step 90° switching process. The coercive field required for a multistep switching process can be decreased by about 50% in comparison to that for single domains. The approach of reducing the electric field presents significant opportunities for the design and enhancement of devices based on ferroelectric materials across various applications.

DOI: [10.1103/PhysRevB.109.214101](https://doi.org/10.1103/PhysRevB.109.214101)**I. INTRODUCTION**

Ferroelectric thin films exhibit immense promise for applications in nonvolatile memories and electronic nanodevices owing to their notable characteristics such as switchable spontaneous polarizations, high dielectric susceptibility [1,2], and large piezoelectric strains [3,4]. However, due to persistent issues such as fatigue, temperature stability, and dielectric breakdown [5,6], reducing the coercive field is fundamental to optimizing the performance and reliability of ferroelectric thin film devices with lower energy consumption, faster switching speed, and enhanced device reliability [7,8].

The coercive electric field E_c , which represents the minimum electric field required to switch the polarization, is typically determined by analyzing the polarization–electric field hysteresis loops of ferroelectric thin films [9]. In particular, the polarization evolution and switching process, highly dependent on the phase and domain patterns, can significantly affect the corresponding coercive fields [10]. Additionally, E_c also varies with frequency [11,12], film thickness [13], domain pinning [14], crystal orientation [15], temperature [16], surface boundary conditions [17,18], and the built-in depolarization field [19,20]. To sufficiently reduce the coercive field in ferroelectric nanodevices, it is essential to understand polarization switching behaviors and tailor the domain structures for fast speed and low leakage ferroelectric devices.

It is widely accepted that E_c in ferroelectric thin films can be greatly reduced by manipulating the phase and domain structures [10,15]. Particularly, recent studies show that strain engineering has emerged as a promising route to induce phase competition for large electromechanical responses

and low driving voltage [10,21–23]. For example, a broad coercive field distribution is achieved in a 4 nm epitaxial PbZr_{0.48}Ti_{0.52}O₃ film by driving the system towards instability at the morphotropic phase boundary [21]. The coercive field in epitaxial BiFeO₃ thin films can be reduced by up to 60% due to strain-induced mixed-phase coexistence [22]. A two-step ferroelastic switching process is observed in 40 nm PbTiO₃ films with an initial a_1/a_2 stable state. c domains can be formed by using a bias pattern (175 MV/m), and then can be erased back to the a_1/a_2 state by using interdigitated electrodes with an electric field of 10 MV/m, corresponding to a voltage of only 0.4 V [10]. Alternatively, the polarization switching process from the out of plane to the in-plane direction by a vertical electric field is first realized in epitaxial 70 nm PbTiO₃ thin films, and the driving out of plane voltage from c/a domains to a_1/a_2 domains is 2 V, corresponding to the coercive field of 28.5 MV/m [23]. Despite diverse experimental observations and measurements of P - E loops, the driving voltage in ferroelectric thin films still requires more theoretical study, especially in systems with complex ferroelectric domains [21–23].

The coercive field was first theoretically studied in 1934 by Mueller, who proposed a phenomenological theory for Rochelle salt [24]. Devonshire further modified the theory in 1949 for BaTiO₃ crystals with the consideration of elastic and electromechanical effects [25]. The coercive field was found to be crucially dependent on the domain switching mechanisms [24–36], including the influence of domain pinning [26], preexisting domain walls [27], and mechanical strains [28]. The Landau's phenomenological theory was also used to predict the polarization switching path under boundary conditions [29,30]. Particularly, the intrinsic coercive field of 90° domain switching of BaTiO₃ single crystals was investigated, and results show that 180° polarization switching under

^{*}luxy@hit.edu.cn

an external electric field of 8 MV/m can be accomplished by a two-step 90° polarization switching under an external tensile stress of 140 MPa [30]. However, the obtained theoretical predictions of coercive fields are often higher than experimental observations by two orders of magnitude or more [26–30].

The nucleation theory was also developed to describe the polarization process in ferroelectric bulks [31,32]. Merz [31] and Landauer [32] considered domain wall mobility and nucleation under an external electric field, and then derived the minimum activation energy of nucleated domains to calculate the corresponding critical electric fields in BaTiO₃ single crystals. However, the calculated activation energy and corresponding coercive field are still three orders higher than the experiment results. The discrepancy is also called the “Landauer paradox” [32]. To avoid this paradox, the effect of inhomogeneous defects [33], domain wall thickness [34], and ferroelectric-electrode coupling [35] were considered within the activation energy of nuclei. A general form of the energy release rate for the dynamic movement process of a switched 180° domain wall under an external electric field was further proposed by Wang and Xiao [36]. The estimated coercive (critical) field is about 0.22 MV/m which is consistent with the experiment results for BaTiO₃ crystals [36]. However, the nucleation theory is limited in the application of non-180° domain switching.

For ferroelectric thin films, it is well known that the extrinsic coercive fields of thin films are much higher than those of the bulk’s counterparts due to the size effect of nucleation [37,38]. For example, the measured coercive field is 1.5 MV/m for a 400 nm thick BaTiO₃ film and 0.15 MV/m for bulk single crystal [37], even though the intrinsic E_c for thin films predicted by using Landau’s phenomenological theory is still one or two orders higher than the observed experiment results in thin films [38]. The closest one is the coercive field of 500 MV/m in ultrathin vinylidene fluoride copolymer films with a thickness of less than 15 nm fabricated by Langmuir-Blodgett deposition [39]. In addition, the intrinsic E_c predicted by Pertsev *et al.* is also close to the measured coercive field ranging from 90 to 20 MV/m for Pb(Zr_{0.52}Ti_{0.48})O₃ epitaxial films with thickness ranging from 10 to 100 nm, and both intrinsic and extrinsic coercive fields strongly depend on compressive substrate strains [40].

Piezoresponse force microscopy (PFM) is a power tool to probe the local coercive field of thin films [10,41]. Kalinin *et al.* proposed a point charge model to describe the local switching behavior by PFM and found that the local coercive (critical) field of 180° domain switching increases with switched domain sizes [42]. To describe the

formation of 90° domains by PFM tip fields as observed in PbTiO₃ [10], Pb(Zr_{0.1}Ti_{0.9})O₃ [43], and Pb(Zr_{0.2}Ti_{0.8})O₃ thin films [44], Chen *et al.* proposed an isotropic thermodynamic criterion for ferroelastic 90° domain switching to evaluate the relaxation of surface piezostress during the switching process [45]. However, the predicted coercive field is still much higher than experimental measurements due to the neglected twinning structures and the interface interactions [45].

Domain twinning and the interface elastic interaction can significantly affect the domain switching and the coercive field in ferroelectric thin films, especially with multiple phases/domains near phase boundaries [46–48]. Phase and domain coexistence can greatly decrease the driving voltage due to the synergetic and/or multistep switching process in ferroelectric thin films under particular conditions [10,21–23]. A 180° domain switching process could be favored by two 90° switching processes near the phase boundary between the twinned c/a and a_1/a_2 phases [23]. However, it is still a challenge to theoretically predict the coercive field in such systems due to the complex coexisting domain structures.

In this work, we theoretically study the ferroelastic switching process and the coercive fields in epitaxial PbTiO₃ thin films within the framework of Landau’s phenomenological theory. The elastic interaction of the polydomain of c/a and a_1/a_2 domains is considered to predict the coercive field of epitaxial ferroelectric thin films under various substrate strains.

II. MULTISTEP SWITCHING OF COEXISTING DOMAINS

In this section, we focus on the (001)-oriented PbTiO₃ film epitaxially grown on a cubic substrate with a surface parallel to the (001) crystallographic planes. The ferroelectric film usually has multiphases or polydomain states. However, we will start from a single domain state for simplicity, and then discuss and compare each possible condition. We assume the film is epitaxially uniform with a transversely isotropic misfit strain, and the influence of the depolarization field is neglected.

A. Ferroelastic switching of single domains

For films with tetragonal phase, domains with out of plane polarization and in-plane polarization are noted as c domain and a domain, respectively. The renormalized thermodynamic potential after the Legendre transformation of the Gibbs free energy is expressed with respect to the primary order parameters of polarization P_i and internal mechanical stresses σ_i in the film as follows [49],

$$\begin{aligned}
 F = & a_1(P_1^2 + P_2^2 + P_3^2) + a_{11}(P_1^4 + P_2^4 + P_3^4) + a_{12}(P_1^2 P_2^2 + P_2^2 P_3^2 + P_3^2 P_1^2) \\
 & + a_{111}(P_1^6 + P_2^6 + P_3^6) + a_{112}[P_1^2(P_2^4 + P_3^4) + P_2^2(P_3^4 + P_1^4) + P_3^2(P_1^4 + P_2^4)] \\
 & + a_{123}P_1^2 P_2^2 P_3^2 - \frac{1}{2}s_{11}(\sigma_1^2 + \sigma_2^2 + \sigma_3^2) - s_{12}(\sigma_1\sigma_2 + \sigma_2\sigma_3 + \sigma_1\sigma_3) - \frac{1}{2}s_{44}(\sigma_4^2 + \sigma_5^2 + \sigma_6^2) \\
 & - Q_{11}(\sigma_1 P_1^2 + \sigma_2 P_2^2 + \sigma_3 P_3^2) - Q_{12}[\sigma_1(P_2^2 + P_3^2) + \sigma_2(P_1^2 + P_3^2) + \sigma_3(P_1^2 + P_2^2)] \\
 & - Q_{44}(P_2 P_3 \sigma_4 + P_1 P_3 \sigma_5 + P_2 P_1 \sigma_6) + (\sigma_1 S_1 + \sigma_2 S_2) - P_1 E_1 - P_2 E_2 - P_3 E_3,
 \end{aligned} \tag{1}$$

where F is the total free energy; a_i , a_{ij} , and a_{ijk} are the linear and nonlinear dielectric stiffness coefficients; s_{ij} and Q_{ij} are the elastic compliances and the electrostrictive coefficients, respectively; E_i is the external electric field. Parameters of PbTiO₃ for the calculations are taken from Ref. [49].

The stress components in Eq. (1) can be solved with the mechanical conditions of the film/substrate system: $\partial F/\partial \sigma_1 = \partial F/\partial \sigma_2 = -u_m$, $\partial F/\partial \sigma_6 = 0$, and $\sigma_3 = \sigma_4 = \sigma_5 = 0$, where u_m is substrate strain [49]. The Gibbs free energy including the Landau free energy, elastic energy, and electrostatic energy provided by the out of plane electric field can be therefore derived as follows [49],

$$\begin{aligned}
 F = & a_1^*(P_1^2 + P_2^2) + a_3^*P_3^2 + a_{11}^*(P_1^4 + P_2^4) + a_{33}^*P_3^4 \\
 & + a_{13}^*(P_1^2P_2^2 + P_2^2P_1^2) \\
 & + a_{12}^*P_1^2P_2^2 + a_{111}(P_1^6 + P_2^6 + P_3^6) + a_{123}P_1^2P_2^2P_3^2 \\
 & + a_{112}[P_1^4(P_2^2 + P_3^2) + P_2^4(P_1^2 + P_3^2) + P_3^4(P_1^2 + P_2^2)] \\
 & + \frac{u_m^2}{s_{11} + s_{12}} - E_3P_3, \quad (2)
 \end{aligned}$$

where $a_1^* = a_1 - u_m(Q_{11} + Q_{12})/(s_{11} + s_{12})$, $a_{11}^* = a_{11} + [(Q_{11}^2 + Q_{12}^2)s_{11} - 2Q_{11}Q_{12}s_{12}]/(2s_{11}^2 + 2s_{12}^2)$, $a_{13}^* = a_{12} + Q_{12}(Q_{11} + Q_{12})/(s_{11} + s_{12})$, $a_{12}^* = a_{12} - [(Q_{11}^2 + Q_{12}^2)s_{12} - 2Q_{11}Q_{12}s_{11}]/(s_{11}^2 + s_{12}^2) + Q_{44}^2/(2s_{44})$, $a_3^* = a_1 - 2u_mQ_{12}(s_{11} + s_{12})$, and $a_{33}^* = a_{11} + Q_{12}^2/(s_{11} + s_{12})$. Noting that the P_2 can be neglected as zero due to in-plane mechanical symmetry, the reduced expression can be written as follows [49]:

$$\begin{aligned}
 F = & a_1^*P_1^2 + a_3^*P_3^2 + a_{11}^*P_1^4 + a_{33}^*P_3^4 + a_{13}^*P_1^2P_3^2 \\
 & + a_{111}(P_1^6 + P_3^6) + a_{112}(P_1^4P_3^2 + P_3^4P_1^2) \\
 & + \frac{u_m^2}{s_{11} + s_{12}} - E_3P_3. \quad (3)
 \end{aligned}$$

We focus on the domain switching process during the tensile strain regime of 0%–0.8%, where different domain structures coexist [10,21–23]. As shown in the energy landscape for films under a substrate strain of 0% [Fig. 1(a)] without electric field, c domains have a lower value of energy well and are more stable than a domains, while a domains dominate under a tensile substrate strain of 0.8% [Fig. 1(b)], which is consistent with experimental observations [10].

To investigate the switching behavior of c domains, the $F - P_3$ curves obtained by extracting the minimum value of total free energy with respect to P_3 are studied, as shown in Fig. 2. In contrast with typical $F - P$ curves with only two stable energy wells, the free energy curves show a distinct triple energy well even under zero field [50]. This extra well represents the stable existence of a domains.

With the increase of vertical electric fields, the free energy potentials show different switching behaviors in these two films with different substrates. As shown in Figs. 2(a) and 2(b) for the film under a substrate strain of 0%, the energy well of c^- domains becomes a saddle point [red point in Fig. 2(c)], indicating a 180° switching process from c^- domains to c^+ domains under 0, 12.4, and 109.4 MV/m. Therefore, 109.4 MV/m is considered as the 180° coercive field E_c^{180} of c domains. However, for the film under a substrate strain of

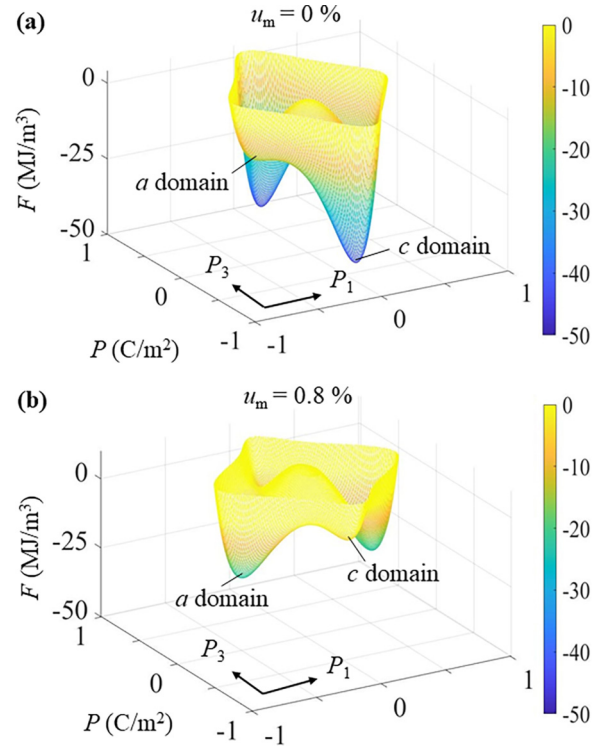


FIG. 1. The Gibbs free energy profile of single domains under misfit strain of (a) 0% and (b) 0.8%.

0.8% as shown in Figs. 2(d)–2(f), the c^- domains switch to a domains when the electric field increases to 45.2 MV/m, and further switch to c^+ domains at 88.8 MV/m, indicating a two-step 90° switching process. We consider 45.2 and 88.8 MV/m in this case is the 90° and 180° coercive field E_c^{90} and E_c^{180} of c domains, respectively. It is worthwhile noting that the switching behaviors and coercive field of c domains strongly depend on the substrate strains.

To further study the substrate dependence of the switching behaviors, the variation of E_c^{180} and E_c^{90} of c domains with misfit strain is further calculated, as shown in Fig. 3. When

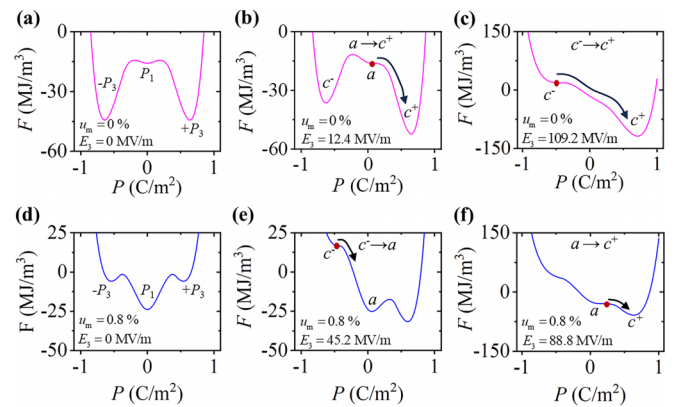


FIG. 2. The landscape of total free energies of single domains in PbTiO₃ epitaxial thin films with substrate strains of 0% and 0.8%. The $F - P_3$ curves at electric fields of (a) 0, (b) 12.4, and (c) 109.2 MV/m under a misfit strain of 0%. $F - P_3$ curves at electric fields of (d) 0, (e) 45.2, and (f) 88.8 MV/m under a misfit strain of 0.8%.

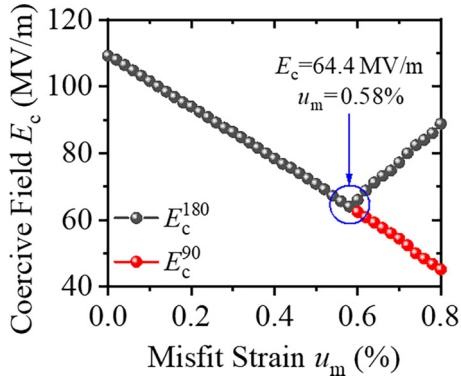


FIG. 3. Strain dependence of coercive fields E_c^{180} and E_c^{90} of c domains.

the misfit strain exceeds 0.58%, the E_c^{90} appears and decreases with increasing tensile strain. This strain-dependence variation can be explained by the stability of a domains [49]. We note that this critical strain of 0.58% is slightly larger than the a_1/a_2 and c/a domain boundary [49] without the consideration of the elastic coupling effect of the polydomain, which will be considered in the next section. The existence of E_c^{90} indicates the transition of the switching process from one 180° switching ($c^- \rightarrow c^+$) to two 90° switching ($c^- \rightarrow a \rightarrow c^+$) under vertical electric fields. On the other hand, there is a minimum E_c^{180} value of 64.0 MV/m near the substrate strain of 0.58%, which is near the phase boundary of PbTiO_3 thin films [49]. Compared with the coercive field of c domains under compressive strain, the E_c^{180} is reduced by about 50% (from 125.6 to 64.4 MV/m) via strain engineering.

B. Multistep switching of polydomains

The combination of a domains and c domains is noted as c/a domains, and that of the perpendicular a domains is noted as a_1/a_2 domains. Due to the existence of a domains and the elastic coupling in polydomains of c/a and a_1/a_2 domains, the coercive field could be different from those single domains. Therefore, it is necessary to build a theoretical model for ferroelectric films with possible existing c/a and a_1/a_2 domains, as shown in the schematic of Fig. 4.

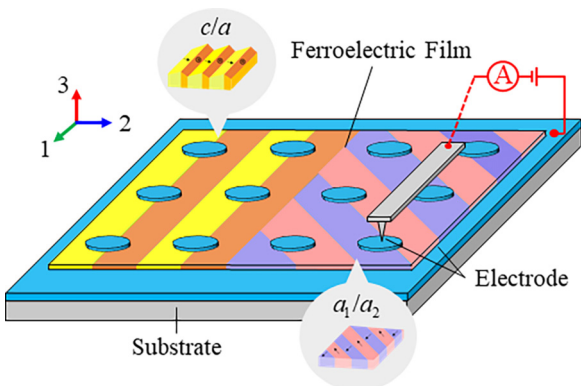


FIG. 4. Schematic illustration of polydomain films with a_1/a_2 and c/a domain structures.

For epitaxial polydomain films, the mean in-plane strains $\langle S_1 \rangle$, $\langle S_2 \rangle$ are equal to the substrate strain u_m , and the shear strains and shear stresses are ignored with $\langle S_6 \rangle = 0$ and $\langle \sigma_4 \rangle = \langle \sigma_5 \rangle = 0$. On the film surface, the mean of out of plane stress is also considered as zero, i.e., $\langle \sigma_3 \rangle = 0$.

For c/a domains, we assume the polarizations of a and c domains are equal to the spontaneous polarization $|P_1^a| = |P_3^c| = P_s$, and other components are zero without an electric field. The mechanical compatibility between c and a domains is considered as $S_i^a(1 - \varphi_c) + S_i^c \varphi_c = S_i$, ($i = 1, 2, 6$), and $\sigma_i^a = \sigma_i^c = 0$ ($i = 3-6$), where φ_c is the volume fraction of the c domains in c/a domains; σ_i^c , σ_i^a , S_i^c , and S_i^a are stress and strain of a and c domains in c/a domains [51]. Ignore the shear strain for simplicity, the in-plane normal strain of c and a domains can be derived by mechanical compatibility $S_1^a = u_m + \varphi_c(Q_{11} - Q_{12})P_s^2$ and $S_1^c = u_m - (1 - \varphi_c)(Q_{11} - Q_{12})P_s^2$ [49]. The corresponding internal stress of c domains can be further derived as $\sigma_1^c = [(s_{11} - s_{12})u_m - (s_{11}Q_{11} - s_{12}Q_{12})P_s^2 + s_{11}(Q_{11} - Q_{12})P_s^2\varphi_c] / (s_{11}^2 - s_{12}^2)$ and $\sigma_2^c = (u_m - Q_{12}P_s^2 - s_{12}\sigma_1^a) / s_{11}$; the internal stress of a domains is equal to c domains $\sigma_1^a = \sigma_1^c$ and $\sigma_2^a = \sigma_2^c$.

Under electric field E_3 , the total free energy of c/a domains can be expressed by $F_{c/a} = \varphi_c F_c + (1 - \varphi_c) F_a$, where F_c and F_a can be written as follows [51]:

$$F_a = a_1(P_1^2 + P_3^2) + a_{12}P_1^2P_3^2 + a_{11}(P_1^4 + P_3^4) + a_{111}(P_1^6 + P_3^6) + a_{112}(P_1^4P_3^2 + P_1^2P_3^4) - \frac{1}{2}s_{11}[(\sigma_1^a)^2 + (\sigma_2^a)^2] - s_{12}\sigma_1^a\sigma_2^a - Q_{11}P_3^2\sigma_1^a - Q_{12}(P_1^2 + P_3^2)\sigma_2^a + S_1^a\sigma_1^a + S_2^a\sigma_2^a, \quad (4)$$

$$F_c = a_1(P_1^2 + P_3^2) + a_{12}P_1^2P_3^2 + a_{11}(P_1^4 + P_3^4) + a_{111}(P_1^6 + P_3^6) + a_{112}(P_1^4P_3^2 + P_1^2P_3^4) - \frac{1}{2}s_{11}[(\sigma_1^c)^2 + (\sigma_2^c)^2] - s_{12}\sigma_1^c\sigma_2^c - Q_{12}P_3^2\sigma_1^c - Q_{12}(P_1^2 + P_3^2)\sigma_2^c + S_1^c\sigma_1^c + S_2^c\sigma_2^c - E_3P_3. \quad (5)$$

The total free energy density $F_{c/a}$ can be expressed by φ_c , P_1 , and P_3 , where the equilibrium fraction φ_c^* of c domains in c/a domains can be derived from $\partial F_{c/a} / \partial \varphi_c = 0$,

$$\varphi_c^* = 1 - \frac{(s_{11} - s_{12})(u_m - Q_{12}P_3^2)}{s_{11}(Q_{11} - Q_{12})P_3^2} + \frac{E_3(s_{11}^2 - s_{12}^2)}{2s_{11}(Q_{11} - Q_{12})^2P_3^3}. \quad (6)$$

Therefore, the stable total free energy of c/a domains is $F_{c/a} = \varphi_c^* F_c + (1 - \varphi_c^*) F_a$.

The switching behavior of c/a domains can be collective with complex switching dynamics [23]. Here, for simplicity, we consider the final state with switched c and a domains in c/a domains under the applied vertical field, which can be probed by minimizing the total free energy and examining the lowest energy well during the domain switching. Using Eqs. (4) and (5) without an electric field, the total free energy landscape of the c domain and a domains in c/a domains is shown in Fig. 5. The energy barriers between c and a domains are labeled with purple lines. Under the tensile strain of 0.46%, the energy wells of c domains and a domains are

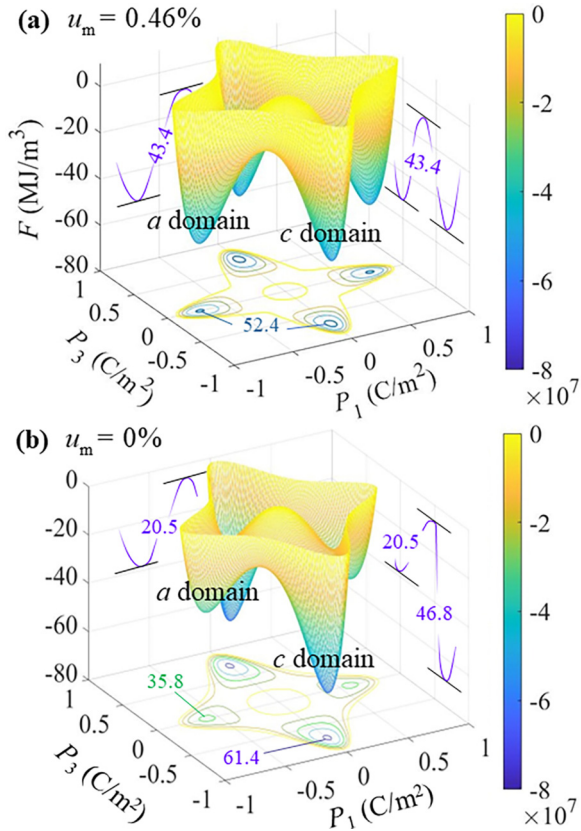


FIG. 5. The Gibbs free energy profile of ca domains PbTiO₃ films under misfit strains of (a) 0.46% and (b) 0%.

equal, indicating the metastable state of coexisting ca and a_1/a_2 domains in films [52]. With the misfit strain decreasing to 0%, ca domains become more stable with lower values of the energy well due to the stability of c domains. Compared with single c domains, the ca domains have lower potential wells under the same substrate strain, which is compatible with the experimental observation that ca domains are dominant in PbTiO₃ films other than pure c domains under zero tensile strain [52].

To find the lowest polarization switching path and the switching behaviors under an external electric field, we contour map the total free energy under various E_3 as shown in Fig. 6(a). It is obvious that there are three local minimums under zero field corresponding to the c^- , a , and c^+ domains. For c domains in ca domains, the minimum value of c^- domains rises and becomes saddle points with the applied positive electric field, indicating 90° switching from c^- to a domains. Then the minimum value of a domains further becomes saddle points, indicating a 90° switching process from a to c^+ domains. The schematic of the two-step 90° switching process of ca domains is indicated in Fig. 6(b). Further, we extract the total free energy profile along the lowest value with respect to P_3 shown in Fig. 6(b). The extracted path of energy profiles in Fig. 6(b) corresponds to the lines and arrows in Fig. 6(a) in the same color. To find this change and the saddle points indicated by black arrows in Fig. 6(b), we give the first-order derivative $F_{c/a}$ with respect to P_3 as shown in Fig. 6(c). When ferroelastic switching occurs, we have the

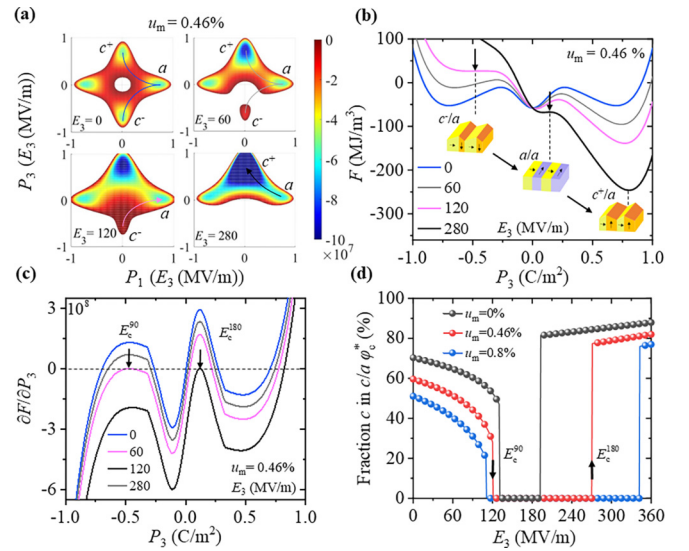


FIG. 6. The switching behaviors of ca domains in PbTiO₃ epitaxial thin films. (a) Contour map of free energy, (b) free energy with respect to P_3 , and (c) first-order deviation of free energy under misfit strain of 0.46% with applied electric fields of 0, 60, 120, and 280 MV/m. (d) The volume function of c domains in ca domains with respect to electric field with misfit strain u_m of 0%, 0.46%, and 0.8%.

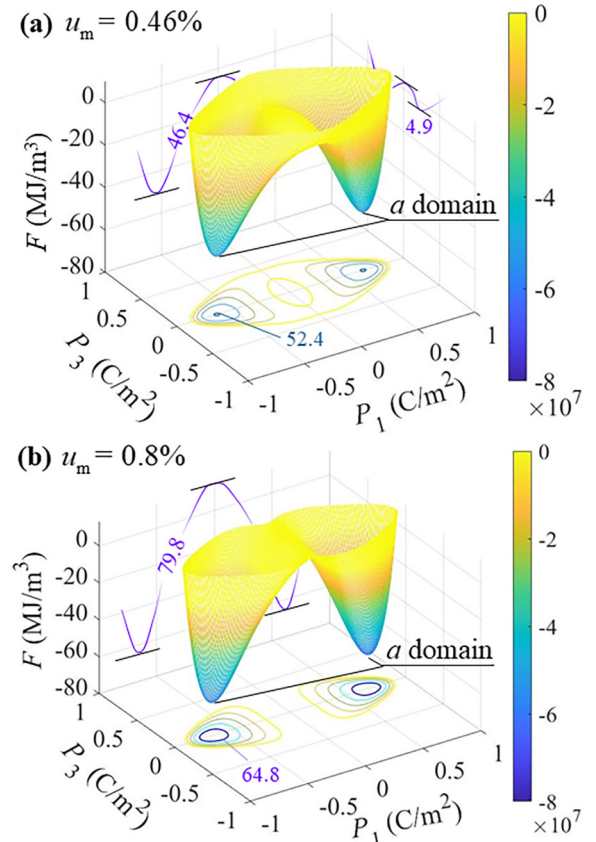


FIG. 7. The Gibbs free energy profile of a_1/a_2 domains PbTiO₃ films under different misfit strains of (a) 0.46% and (b) 0.8%.

local minimums with $\partial F_{c/a}/\partial P_3 = 0$ and $\partial^2 F_{c/a}/\partial^2 P_3 > 0$. The obtained critical electric field of 120 and 280 MV/m can be considered as the coercive field of E_c^{90} and E_c^{180} for c^- domains switching to a domains and c^+ domains, respectively. Similarly, a domains in c/a domains switch to c domains at 280 MV/m, which can be considered as the E_c^{90} of a domains.

Moreover, the morphology of c/a domains varies during the switching process. As shown in Fig. 6(d), the variation of c domain fraction φ_c^* with misfit strain and electric field implies the interconversion between c and a domains in c/a domains. When $\varphi_c^* = 0$, all c^- domains switch to a domains, and the fraction of switched a domains increases with misfit strains [51].

For a_1/a_2 domains, similarly, the mechanical compatibility between a_1 and a_2 domains can be expressed as $S_i^{a_1}\varphi_{a_1} + S_i^{a_2}(1 - \varphi_{a_1}) = S_i$ ($i = 1, 2, 6$) and $\sigma_i^{a_1} = \sigma_i^{a_2} = 0$ ($i = 3-6$), where $\sigma_i^{a_1}$, $\sigma_i^{a_2}$, $S_i^{a_1}$, and $S_i^{a_2}$ are the stress and strain of a_1 and a_2 domains; φ_{a_1} is the volume fraction of the a_1 domains [51]. The polarization of a_1 and a_2 domains $|P_1^{a_1}| = |P_2^{a_2}| = P_s$ and $P_1^{a_2} = P_2^{a_1} = 0$. In particular, $|P_3^{a_1}| = |P_3^{a_2}| = P_3 \neq 0$ under vertical electric fields. The strain and stress of a_1 and a_2 domains in the polydomain a_1/a_2 state can be derived as $S_1^{a_1} = S_2^{a_2} = u_m + \varphi_{a_1}(Q_{11} - Q_{12})P_1^2 - Q_{12}P_3^2$,

$$S_1^{a_2} = S_2^{a_1} = u_m - \varphi_{a_1}(Q_{11} - Q_{12})P_1^2 - Q_{12}P_3^2,$$

$$\sigma_1^{a_1} = \sigma_1^{a_2} = (u_m - Q_{11}P_1^2 - Q_{12}P_3^2)/(s_{11} + s_{12})$$

$$+ [s_{11}(1 - \varphi_{a_1}) - s_{12}\varphi_{a_1}](Q_{11} - Q_{12})P_1^2/(s_{11}^2 - s_{12}^2),$$

$$\text{and } \sigma_2^{a_1} = \sigma_2^{a_2} = \sigma_1^{a_1} + [(2\varphi_{a_1} - 1)(Q_{11} - Q_{12})P_1^2 - Q_{12}P_3^2] / (s_{11} - s_{12}).$$

The total free energy of a_1/a_2 domains can be written as $F_{a_1/a_2} = \varphi_{a_1}F_{a_1} + (1 - \varphi_{a_1})F_{a_2}$, where the F_{a_1} and F_{a_2} can be derived as follows [51]:

$$\begin{aligned} F_{a_1} = & a_1(P_1^2 + P_3^2) + a_{12}P_1^2P_3^2 + a_{11}(P_1^4 + P_3^4) \\ & + a_{111}(P_1^6 + P_3^6) + a_{112}(P_1^4P_3^2 + P_1^2P_3^4) \\ & - \frac{1}{2}s_{11}(\sigma_1^{a_1})^2 - \frac{1}{2}s_{11}(\sigma_2^{a_1})^2 \\ & - s_{12}\sigma_1^{a_1}\sigma_2^{a_1} - Q_{11}P_3^2\sigma_1^{a_1} - Q_{12}(P_1^2 + P_3^2)\sigma_2^{a_1} \\ & + S_1^{a_1}\sigma_1^{a_1} + S_2^{a_1}\sigma_2^{a_1} - E_3P_3, \end{aligned} \quad (7)$$

$$\begin{aligned} F_{a_2} = & a_1(P_1^2 + P_3^2) + a_{12}P_1^2P_3^2 + a_{11}(P_1^4 + P_3^4) \\ & + a_{111}(P_1^6 + P_3^6) + a_{112}(P_1^4P_3^2 + P_1^2P_3^4) \\ & - \frac{1}{2}s_{11}(\sigma_1^{a_2})^2 - \frac{1}{2}s_{11}(\sigma_2^{a_2})^2 - s_{12}\sigma_1^{a_2}\sigma_2^{a_2} - Q_{11}P_3^2\sigma_1^{a_2} \\ & - Q_{12}(P_1^2 + P_3^2)\sigma_2^{a_2} + S_1^{a_2}\sigma_1^{a_2} + S_2^{a_2}\sigma_2^{a_2} - E_3P_3. \end{aligned} \quad (8)$$

The total free energy density F_{a_1/a_2} is, therefore, the function of φ_{a_1} , P_1 , and P_3 . The equilibrium fraction $\varphi_{a_1}^*$ can be derived from $\partial F_{a_1/a_2}/\partial \varphi_{a_1} = 0$, resulting in $F_{a_1} = F_{a_2}$, i.e., $\varphi_{a_1}^* = 50\%$. The stable total free energy of a_1/a_2 domains can be expressed as $F_{a_1/a_2} = \varphi_{a_1}^*F_{a_1} + (1 - \varphi_{a_1}^*)F_{a_2}$.

The switching behavior of a_1/a_2 domains is also studied as shown in Fig. 7. Different from the c/a domains, there are only two energy wells representing the a_1 or a_2 domains [52]. The contour in Fig. 7 exhibits in-plane barriers between two opposite a domains. The in-plane barrier decreases with decreasing tensile strain due to the instability of the a

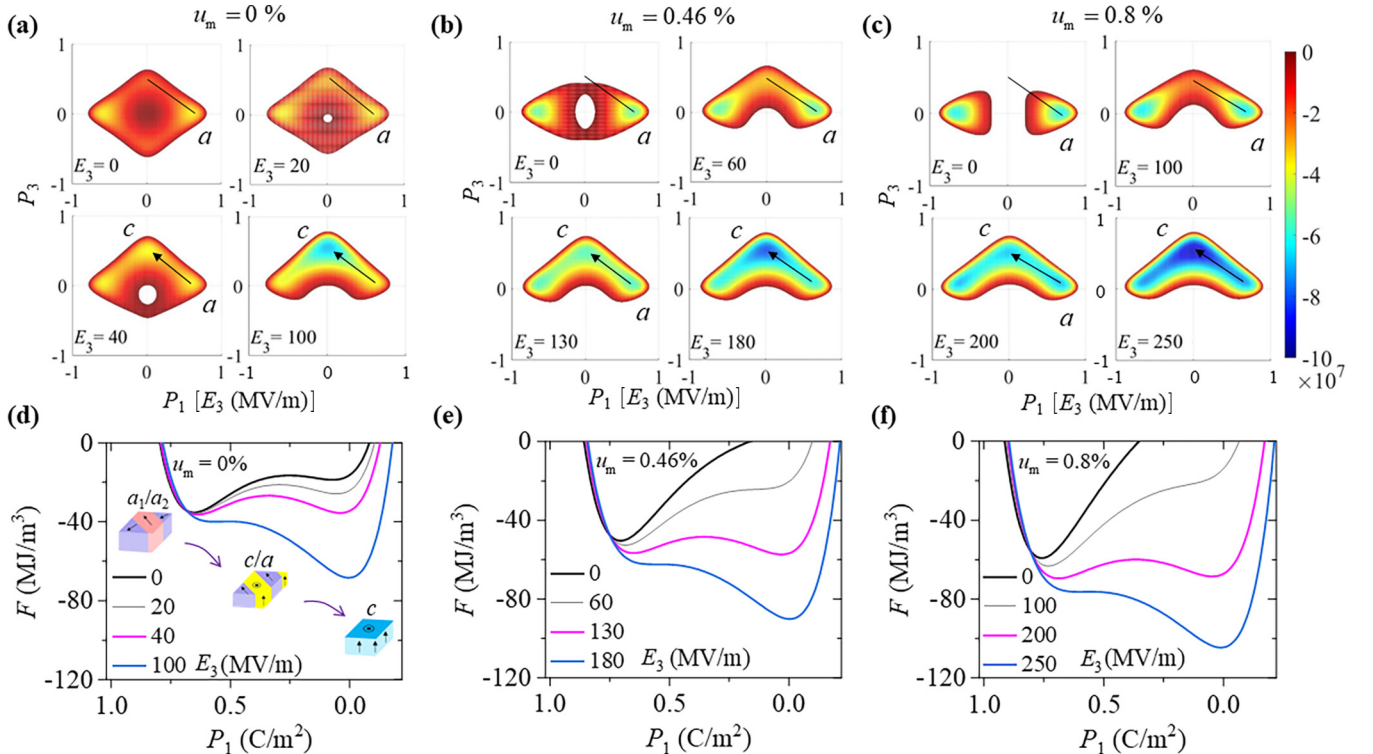


FIG. 8. The switching behaviors of a_1/a_2 domains in PbTiO_3 epitaxial thin films under typical substrate strains. Contour maps of free energy for a_1/a_2 domains under misfit strains of (a) 0%, (b) 0.46%, and (c) 0.8%, and energy profiles with respect to P_1 under misfit strains of (d) 0%, (e) 0.46%, and (f) 0.8%. The insets in (d) illustrate the switching process of a_1/a_2 domains under electric field E_3 .

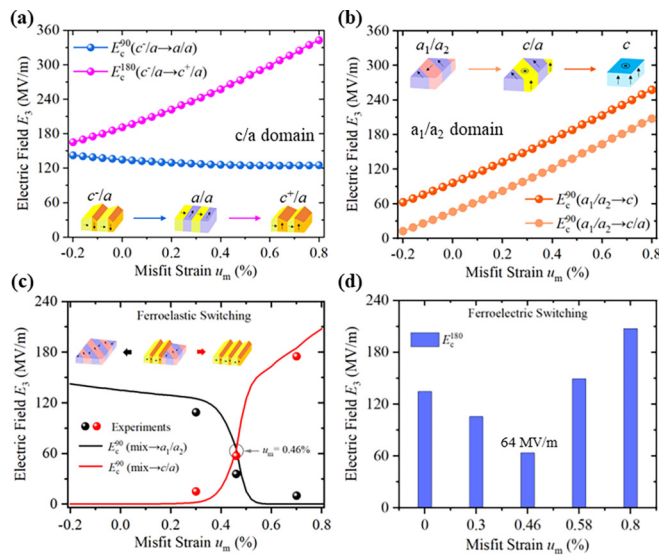


FIG. 9. The substrate strain-dependent switching behaviors of coexisting polydomains in PbTiO_3 epitaxial thin films. Coercive fields of (a) c/a domains, and (b) a_1/a_2 domains vary with substrate strains. (c,d) are average coercive fields of ferroelastic and ferroelectric switching of coexisting polydomains, respectively. Experiment results from Refs. [10,17,23] in (c) are noted by red and black points in (c) for comparison. The inserts in (a–c) illustrate the switching process of c/a , a_1/a_2 , and coexisting polydomains.

domains. The lateral switching behavior between two a domains can be driven by the in-plane electric field, as illustrated in earlier studies [53]. The decrease of the in-plane barrier suggests the in-plane driving voltage could be reduced by strain engineering.

To further study the switching behavior of a_1/a_2 domains under a vertical electric field, the contour maps and the energy profiles extracted along the energy valley with respect to P_1

are shown in Fig. 8. The extracted path is shown with lines and arrows in Figs. 8(a)–8(c). The existing a_1/a_2 domains switch to c domains to form a c/a domain structure, which is similar within the strain regime of 0%–0.8%. Two coercive fields in two-step 90° switching processes increase with tensile strain due to the stability of a domains as shown in Figs. 8(d)–8(f).

The strain dependence of the coercive fields is given in Fig. 9. Results show that both c/a and a_1/a_2 domains experience the two-step ferroelastic switching process near the phase boundary. There are sharp changes for these two coercive fields as shown in Figs. 9(c)–9(d). The average E_c^{90} decreases from 148 MV/m under a substrate strain of 0% to 60 MV/m under the critical substrate strain of 0.46%, which is quite coincident with the experiment results as noted by the black dots in Fig. 9(c). It is the same for E_c^{180} which decreases sharply down to 50% under the misfit strain of 0.46%, implying the easy switching between coexisting domain structures near the phase boundary [23].

In summary, we study the ferroelastic and ferroelectric switching of coexisting domains in ferroelectric lead-titanate thin films within the framework of Landau’s phenomenological theory. The corresponding coercive fields in PbTiO_3 films are compared with the consideration of elastic interactions. Results show that the coercive field can be reduced up to 50% under the critical strain of 0.46%. Our results indicate an efficient way to reduce the coercive field by introducing domain coexistence near the critical boundary.

ACKNOWLEDGMENTS

This work is supported by the National Key Research and Development Program of China (Grant No. 2021YFF0501001), the National Science Foundation of China (Grant No. 12372148), the Fundamental Research Funds for the Central Universities (Grant No. LH2020A006), and Open Fund of Key Laboratory for Intelligent Nano Materials and Devices of the Ministry of Education NJ2022002 (Grant No. INMD-2022M01).

[1] Y. Zhai, A. Fan, K. Zhong, D. Karpinsky, Q. Gao, J. Yi, and L. Liu, Great enhancement of ferroelectric properties of Al_2O_3 -modified BiFeO_3 thin films obtained by sol-gel method, *J. Eur. Ceram. Soc.* **44**, 224 (2024).
 [2] F. Ni, L. Xu, K. Zhu, H. Yan, B. Shen, H. Zeng, and J. Zhai, Improved piezoelectric performance via orientation regulation in novel BNT-BT-SBT thin film, *J. Alloys Compd.* **934**, 167936 (2023).
 [3] O. Paull, C. Xu, X. Cheng, Y. Zhang, B. Xu, K. P. Kelley, A. Marco, R. K. Vasudevan, L. Bellaiche, V. Nagarajan, and D. Sando, Anisotropic epitaxial stabilization of a low-symmetry ferroelectric with enhanced electromechanical response, *Nat. Mater.* **21**, 74 (2023).
 [4] A. Biswas, W. J. Kennedy, N. R. Glavin, and P. M. Ajayan, Epitaxial conducting ABO_3 perovskite oxide thin films, *J. Appl. Phys.* **133**, 240701 (2023).
 [5] R. Bouregba, On the origin of polarization fatigue and Curie-von Schweidler relaxation current in $\text{Pb}(\text{Zr}_x, \text{Ti}_{1-x})\text{O}_3$

ferroelectric thin films: A unique mechanism based on charge trapping by interface defects, *J. Appl. Phys.* **133**, 014101 (2023).
 [6] X. Chen, J. Zhang, B. Huang, Y. Liu, and P. Yu, An artificial dead-layer to protect the ferroelectric thin films from electron injection, *J. Appl. Phys.* **134**, 044103 (2023).
 [7] Y. Wang, L. Tao, R. Guzman, Q. Luo, W. Zhou, Y. Yang, Y. Wei, Y. Liu, P. Jiang, Y. Chen, S. Lv, Y. Ding, W. Wei, T. Gong, Y. Wang, Q. Liu, S. Du, and M. Liu, A stable rhombohedral phase in ferroelectric $\text{Hf}(\text{Zr})_{1+x}\text{O}_2$ capacitor with ultralow coercive field, *Science* **381**, 558 (2023).
 [8] P. Hao, S. Zheng, B. Zeng, T. Yu, Z. Yang, L. Liao, Q. Peng, Q. Yang, Y. Zhou, and M. Liao, Highly enhanced polarization switching speed in HfO_2 -based ferroelectric thin films via a composition gradient strategy, *Adv. Func. Mater.* **33**, 2301746 (2023).
 [9] S. Liu, I. Grinberg, and A. Rappe, Intrinsic ferroelectric switching from first principles, *Nature (London)* **534**, 360 (2023).

- [10] A. R. Damodaran, S. Pandya, J. C. Agar, Y. Cao, R. K. Vasudevan, R. Xu, S. Saremi, Q. Li, J. Kim, M. R. McCarter, L. R. Dedon, T. Angsten, N. Balke, S. Jesse, M. Asta, S. V. Kalinin, and L. W. Martin, Three-state ferroelastic switching and large electromechanical responses in PbTiO_3 thin films, *Adv. Mater.* **29**, 1702069 (2017).
- [11] M. H. Lente, A. Picinin, J. P. Rino, and J. A. Eiras, 90° domain wall relaxation and frequency dependence of the coercive field in the ferroelectric switching process, *J. Appl. Phys.* **95**, 2646 (2004).
- [12] S. Li, D. Zhou, Z. Shi, M. Hoffmann, T. Mikolajick, and U. Schroeder, Involvement of unsaturated switching in the endurance cycling of Si-doped HfO_2 ferroelectric thin films, *Adv. Electron. Mater.* **6**, 2000264 (2020).
- [13] M. Boota, E. P. Houwman, G. Lanzara, and G. Rijnders, Effect of a niobium-doped PZT interfacial layer thickness on the properties of epitaxial PMN-PT thin films, *J. Appl. Phys.* **133**, 145302 (2023).
- [14] T. Jiang, F. Ni, O. Recalde-Benitez, P. Breckner, L. Molina-Luna, F. Zhuo, and J. Rödel, Observation of dislocation-controlled domain nucleation and domain-wall pinning in single-crystal BaTiO_3 , *Appl. Phys. Lett.* **123**, 202901 (2023).
- [15] R. Xu, R. Gao, S. E. Reyes-Lillo, S. Saremi, Y. Dong, H. Lu, Z. Chen, X. Lu, Y. Qi, S. Hsu, A. R. Damodaran, H. Zhou, J. B. Neaton, and L. W. Martin, Reducing coercive-field scaling in ferroelectric thin films via orientation control, *ACS. Nano* **12**, 4736 (2018).
- [16] S. Li, Y. Zhang, J. Ying, Z. Wang, J. Yan, G. Gao, M. Ye, and R. Zheng, Strain-mediated electric-field control of the electronic transport properties of $5d$ iridate thin films of SrIrO_3 , *J. Appl. Phys.* **133**, 014104 (2023).
- [17] E. Langenberg, H. Paik, E. H. Smith, H. P. Nair, I. Hanke, S. Ganschow, G. Catalan, N. Domingo, and D. G. Schlom, Strain-engineered ferroelastic structures in PbTiO_3 films and their control by electric fields, *ACS. Appl. Mater. Interfaces* **12**, 20691 (2020).
- [18] Q. Shi, E. Parsonnet, X. Cheng, N. Fedorova, R. Peng, A. Fernandez, A. Qualls, X. Huang, X. Chang, H. Zhang, D. Pesquera, S. Das, D. Nikonov, I. Yan, L. Chen, L. W. Martin, Y. Huang, J. Íñiguez, and R. Ramesh, The role of lattice dynamics in ferroelectric switching, *Nat. Commun.* **13**, 1110 (2022).
- [19] M. Dawber, P. Chandra, P. B. Littlewood, and J. F. Scott, Depolarization corrections to the coercive field in thin-film ferroelectrics, *J. Condens. Matter. Phys.* **15**, L393 (2003).
- [20] Y. Jiang, E. Parsonnet, A. Qualls, W. Zhao, S. Susarla, D. Pesquera, A. Dasgupta, M. Acharya, H. Zhang, T. Gosavi, C.-C. Lin, D. E. Nikonov, H. Li, I. A. Young, R. Ramesh, and L. W. Martin, Enabling ultra-low-voltage switching in BaTiO_3 , *Nat. Mater.* **21**, 779 (2022).
- [21] M. F. Sarott, M. D. Rossell, M. Fiebig, and T. Morgan, Multilevel polarization switching in ferroelectric thin films, *Nat. Commun.* **13**, 3159 (2022).
- [22] V. Shelke, D. Mazumdar, G. Srinivasan, A. Kumar, S. Jesse, S. Kalinin, A. Baddorf, and A. Gupta, Reduced coercive field in BiFeO_3 thin films through domain engineering, *Adv. Mater.* **23**, 669 (2011).
- [23] X. Lu, Z. Chen, Y. Cao, Y. Tang, R. Xu, S. Saremi, Z. Zhang, L. You, Y. Dong, S. Das, H. Zhang, L. Zheng, H. Wu, W. Lv, G. Xie, X. Liu, J. Li, L. Chen, L. -Q. Chen, W. Cao *et al.*, Mechanical-force-induced non-local collective ferroelastic switching in epitaxial lead-titanate thin films, *Nat. Commun.* **10**, 3951 (2019).
- [24] H. Mueller, Properties of Rochelle salt, *Phys. Rev.* **47**, 175 (1935).
- [25] A. F. Devonshire, XCVI. Theory of barium titanate, *Philos. Mag.* **40**, 1040 (1949).
- [26] Y. Ishibashi and I. Suzuki, The structure, the formation and the activation energies of a domain wall in crystals undergoing the first order transition, *J. Phys. Soc. Jpn.* **53**, 1093 (1984).
- [27] F. Zhuo, X. Zhou, S. Gao, M. Höfling, F. Dietrich, P. B. Groszewicz, L. Fulanović, P. Breckner, A. Wohninsland, B.-X. Xu, H.-J. Kleebe, X. Tan, J. Koruza, D. Damjanovic, and J. Rödel, Anisotropic dislocation-domain wall interactions in ferroelectrics, *Nat. Commun.* **13**, 6676 (2022).
- [28] J. Wang, Y. Li, L.-Q. Chen, and T.-Y. Zhang, The effect of mechanical strains on the ferroelectric and dielectric properties of a model single crystal-phase field simulation, *Acta Mater.* **53**, 2495 (2005).
- [29] Y. W. Li, J. F. Scott, D. N. Fang, and F. X. Li, 90° -Degree polarization switching in BaTiO_3 crystals without domain wall motion, *Appl. Phys. Lett.* **103**, 232901 (2013).
- [30] Y. Li, J. Wang, and F. Li, Intrinsic polarization switching in BaTiO_3 Crystal under uniaxial electromechanical loading, *Phys. Rev. B* **94**, 184108 (2016).
- [31] W. Merz, Domain formation and domain wall motions in ferroelectric BaTiO_3 single crystals, *Phys. Rev.* **95**, 690 (1954).
- [32] R. Landauer, Electrostatic considerations in BaTiO_3 domain formation during polarization reversal, *J. Appl. Phys.* **28**, 227 (1957).
- [33] A. K. Tagantsev, I. Stolichnov, E. L. Colla, and N. Setter, Polarization fatigue in ferroelectric films: Basic experimental findings, phenomenological scenarios, and microscopic features, *J. Appl. Phys.* **90**, 1387 (2001).
- [34] A. M. Bratkovsky and A. P. Levanyuk, Easy collective polarization switching in ferroelectrics, *Phys. Rev. Lett.* **85**, 4614 (2000).
- [35] G. Gerra, A. K. Tagantsev, and N. Setter, Surface-stimulated nucleation of reverse domains in ferroelectrics, *Phys. Rev. Lett.* **94**, 107602 (2005).
- [36] B. Wang and Z. Xiao, On the dynamic growth of a 180° domain in a ferroelectric material, *J. Appl. Phys.* **88**, 1464 (2000).
- [37] K. Iijima, T. Terashima, K. Yamamoto, K. Hirata, and Y. Bando, Preparation of ferroelectric BaTiO_3 thin films by activated reactive evaporation, *Appl. Phys. Lett.* **56**, 527 (1990).
- [38] S. Kim, V. Gopalan, and A. Gruverman, Coercive fields in ferroelectrics: A case study in lithium niobate and lithium tantalate, *Appl. Phys. Lett.* **80**, 2740 (2000).
- [39] S. Ducharme, V. M. Fridkin, A. V. Bune, S. P. Palto, L. M. Blinov, N. N. Petukhova, and S. G. Yudin, Intrinsic ferroelectric coercive field, *Phys. Rev. Lett.* **84**, 175 (2000).
- [40] N. A. Pertsev, J. R. Contreras, V. G. Kukhar, B. Hermanns, H. Kohlstedt, and R. Waser, Coercive field of ultrathin $\text{Pb}(\text{Zr}_{0.52}\text{Ti}_{0.48})\text{O}_3$ epitaxial films, *Appl. Phys. Lett.* **83**, 3356 (2003).
- [41] G. Le Rhun, I. Vrejoiu, L. Pintilie, D. Hesse, M. Alexe, and U. Gösele, Increased ferroelastic domain mobility in ferroelectric thin films and its use in nano-patterned capacitors, *Nanotechnology* **17**, 3154 (2006).
- [42] S. V. Kalinin, A. Gruverman, B. J. Rodriguez, J. Shin, A. P. Baddorf, E. Karapetian, and M. Kachanov,

- Nanoelectromechanics of polarization switching in piezoresponse force microscopy, *J. Appl. Phys.* **97**, 074305 (2005).
- [43] L. Feigl, L. J. McGilly, C. S. Sandu, and N. Setter, Compliant ferroelastic domains in epitaxial $\text{Pb}(\text{Zr}, \text{Ti})\text{O}_3$ thin films, *Appl. Phys. Lett.* **104**, 172904 (2004).
- [44] A. I. Khan, X. Marti, C. Serrao, R. Ramesh, and S. Salahuddin, Voltage-controlled ferroelastic switching in $\text{Pb}(\text{Zr}_{0.2}\text{Ti}_{0.8})\text{O}_3$ thin films, *Nano Lett.* **15**, 2229 (2015).
- [45] L. Chen, J. Ouyang, C. S. Ganpule, V. Nagarajan, R. Ramesh, and A. L. Roytburd, Formation of 90° elastic domains during local 180° switching in epitaxial ferroelectric thin films, *Appl. Phys. Lett.* **84**, 254 (2004).
- [46] S. G. Cao, H.-H. Wu, H. Ren, L.-Q. Chen, J. Wang, J. Li, and T.-Y. Zhang, A novel mechanism to reduce coercive field of ferroelectric materials via $\{111\}$ twin engineering, *Acta Mater.* **97**, 404 (2015).
- [47] K. K. Sahoo, R. Katoch, K. Brajesh, A. Garg, and R. Gupta, Improved ferroelectric response of pulsed laser deposited BiFeO_3 - PbTiO_3 thin films around morphotropic phase boundary with interfacial PbTiO_3 buffer layer, *J. Appl. Phys.* **127**, 064101 (2020).
- [48] T. Shimizu, M. Hasegawa, K. Ishihama, A. Tateyama, W. Yamaoka, R. Tsurumaru, S. Yoshimura, Y. Sato, and H. Funakubo, Large piezoelectric response in lead-free $(\text{Bi}_{0.5}\text{Na}_{0.5})\text{TiO}_3$ -based perovskite thin films by ferroelastic domain switching: Beyond the morphotropic phase boundary paradigm, *ACS Appl. Mater. Interfaces* **13**, 57532 (2021).
- [49] N. Pertsev, A. Zembilgotov, and A. Tagantsev, Effect of mechanical boundary conditions on phase diagrams of epitaxial ferroelectric thin films, *Phys. Rev. Lett.* **80**, 1988 (1998).
- [50] X. Lu, H. Li, and W. Cao, Landau expansion parameters for BaTiO_3 , *J. Appl. Phys.* **114**, 224106 (2013).
- [51] V. G. Kukhar, N. A. Pertsev, H. Kohlstedt, and R. Waser, Polarization states of polydomain epitaxial $\text{Pb}(\text{Zr}_{1-x}\text{Ti}_x)\text{O}_3$ thin films and their dielectric properties, *Phys. Rev. B* **73**, 214103 (2006).
- [52] Y. Dong, X. Lu, J. Fan, S. Y. Choi, and H. Li, Strain engineering of domain coexistence in epitaxial lead-titanite thin films, *Coatings* **12**, 542 (2022).
- [53] S. Matzen, O. Nesterov, G. Rispens, J. A. Heuver, M. Biegalski, H. M. Christen, and B. Noheda, Super switching and control of in-plane ferroelectric nanodomains in strained thin films, *Nat. Commun.* **5**, 4415 (2014).